Oral presentation | Multi-phase flow
High performance computing-I
Tue. Jul 16, 2024 4:30 PM - 6:00 PM Room D

[6-D-02] Ignition Overpressure Analyses of Launch Pads at Different Deflector Angles

Tohid Ghorbani Iriolya[1], *Sinan Eyi[1] (1. Middle East Technical University / Aerospace Engineering Department)

Keywords: Ignition Over Pressure, Launch Pad and Flame Deflector, OpenFOAM

**Twelfth International Conference on
Computational Fluid Dynamics (ICCFD12),
Kobe, Japan, July 14-19, 2024**

Ignition Over-Pressure Analyses of Launch Pads at Different Deflector Angles

T. Ghorbani Iriolya*, S. Eyi*
Corresponding author: tohid.iriolya@metu.edu.tr
* Department of Aerospace Engineering, Middle East Technical University, Ankara 06800, Turkey.

Abstract: The aim of this study is Computational Fluid Dynamics (CFD) analysis of ignition Over-Pressure (IOP) waves. During the ignition of launch vehicle rockets, unsteady pressure waves appear which is called IOP. These waves have high amplitude and low frequencies. IOP waves can have destructive effect on launch vehicle and launch pad. In order to have a safe launch, IOP should be analyzed and nozzle exhaust plume back flow toward launch vehicle should be prevented. In this study, OpenFOAM software is used for flow analyses. Density-based rhoCentralFoam and pressure-based sonicFoam solvers are utilized. The effects of deflector wall angles on IOP waves are investigated using both inviscid and viscous models.

Keywords: Ignition Over-Pressure, Computational Fluid Dynamics, Deflector angle, Inviscid and Viscous Models, Vortex.

1 Introduction

In order to have a safe and successful launch, analyzing the launch environment and designing flame deflectors are necessary. Flame deflectors are facilities that protect the launch pad and launch vehicles from nozzle exhaust plume back flow. During the ignition of engines of the launch vehicle solid rockets, unsteady pressure waves appear which is called Ignition Over-Pressure (IOP). During lift-off, two kinds of pressure waves appear: 1- IOP and 2-Acoustic waves. IOP has higher amplitude and lower frequencies, but acoustic waves have lower amplitude but higher frequencies. The aim of this study is CFD modeling of flame deflectors at different angles. Flow field analysis will be investigated by using unsteady analysis. 2D CFD simulations are done using OpenFOAM software, which is open-source code. Both density-based (rhoCentralFoam) and pressure-based (sonicFoam) compressible solvers were used in this study. Inviscid and viscous Unsteady Reynolds-Averaged Navier-Stokes (URANS) analysis are done. Nance and Liever [1] analytically and experimentally studied acoustic and IOP test for a subscale rocket. They defined IOP as transient phenomena which occurs during launch. Compression of the accelerating nozzle plume, and its propagation and expansion through the exhaust trench and duct holes results in IOP. This high amplitude unsteady flow can adversely affect the launch vehicle and structures. The results show that water injecting systems which do sound suppression, can overcome this phenomenon. Rocket induced vibration and IOP are predicted at low frequencies from 5 to 200 hertz. In order to have successful launch, studying the effects of vibrations and IOP on launch pad and structures are crucial [2]. Canabal et al [3] studied the effect of water injection on the IOP. They used different water injection configurations. Their results show that water injection can strongly affect IOP and also restricts the plume expansion. They reported that increasing the rate of injected water beyond the optimal value does not cause more reduction of the IOP. Lu et al [4] numerically simulated water spray on the launch pad. Two kinds of water systems were used on Long March 7 launch pad. They investigated 3D case with realizable k-e turbulence model. For multiphase analysis they have utilized Eulerian Dispersed Phase (EDP). Results show that first level water spraying system can reduce plume temperature significantly. Because of the nozzle plume back flow, second level water spraying system is also needed. Zhou et al [5] numerically investigated flame deflector design for four liquid engine rockets. For flow analysis, they utilized a compressible form of Reynolds Averaged Navier Stokes (RANS) equations with the realizable k-e turbulence model. Different flow field analysis is done with different impingements and uplift angles. Results show that on the flame deflector surface, high temperatures appear on the impinging point and on the cambered surface. A large impinging angle causes reverse flow while a small impinging angle deflects exhaust gases a little. An appropriate uplift angle can smoothly direct exhaust gases away from

the deflector. The best angle is found to be 25° for impinging angle and 5° for uplift angle. Walsh and Hart [6] evluated IOP for full scale titan launch vehicle. They also have used subscale model of titan and they reported that correlation of subscale with the full scale gives a scaling parameter. Pavish and deese [7] investigated IOP analysis of IOP Delta II and Delta III launch vehicles on launch pad 17B, which was located at Cape Canaveral Air Force Station (CCAFS). Numerical results had good consistency with experimental results. Their results show that both louver and duct control the magnitude and direction of IOP forces. Troclet et al [8] reported that during solid rocket ignition, IOP waves are generated and after that acoustic waves appear. They used an inverse method in order to analyze the launch environment of the ARIANE 5 launch vehicle for identifying IOP sources. Based on literature review, the flame deflector shape and its angle affects IOP and also water injection on nozzle plume can reduce the IOP. In this study, the effect of the variation of deflector angle on IOP will be investigated.

2 Verification Study

In this study the effect of, flame deflector angle on IOP will be investigated, and numerical verification is performed based on the studies of Nonomura et al [9], Tsutsumi et al [10] and Housman et al [11]. They have studied IOP for a 2D case where the deflector angle was 45° and the nozzle exit Mach number and diameter were 2 and 0.1m respectively. Combustion chamber temperature and pressure are 300K and 100000 Pa. Nonomura et al. and Tsutsumi et al. studied IOP effect on sampling point No 10 and Housman et al. studied IOP effect on sampling point No 6. Domain geometry and sampling points are shown in figure 1. All the above-mentioned researchers [9], [10], [11] have investigated IOP on a flat plate at a 45° angle with inviscid simulations. Therefore, verification study for IOP on a flat plate at 45° angle is done based on invisid simulations. Combustion chamber pressure history is the same in studies of Nonomura et al. and Tsutsumi et al. but it is different and higher in Housman et al study. Combustion chamber pressure history is given in figure 2. Boundary conditions for inviscid simulation are shown in table 1.

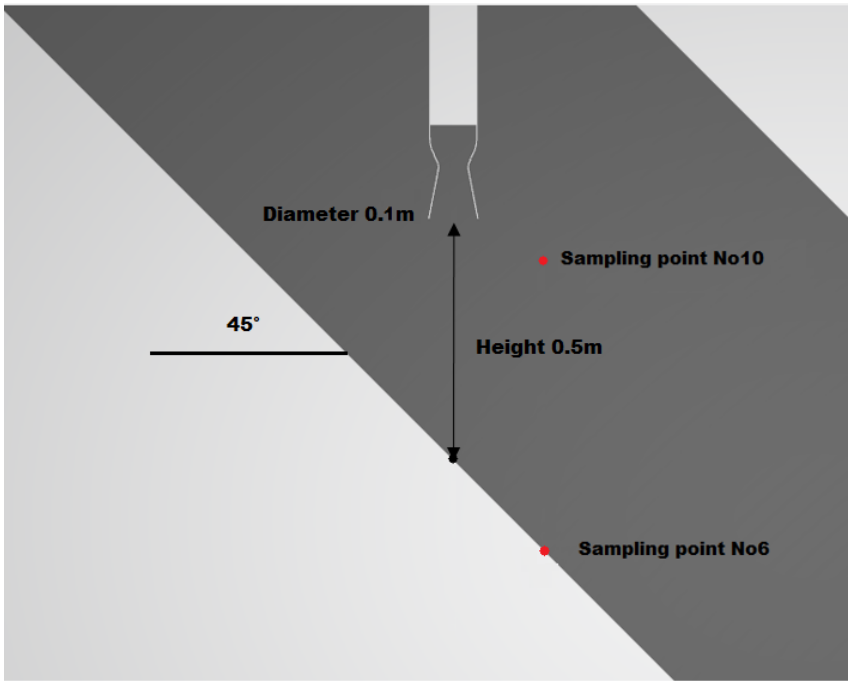

Figure 1: sampling point locations.

In this study for 45° deflector angle, mesh independence study have been done and five kinds of grids with different element sizes have been used. 5mm (Coarser), 4mm (Coarse), 3mm (Medium), 2mm (Fine) and 1.5mm (Finer). Grid information is given in table 2.

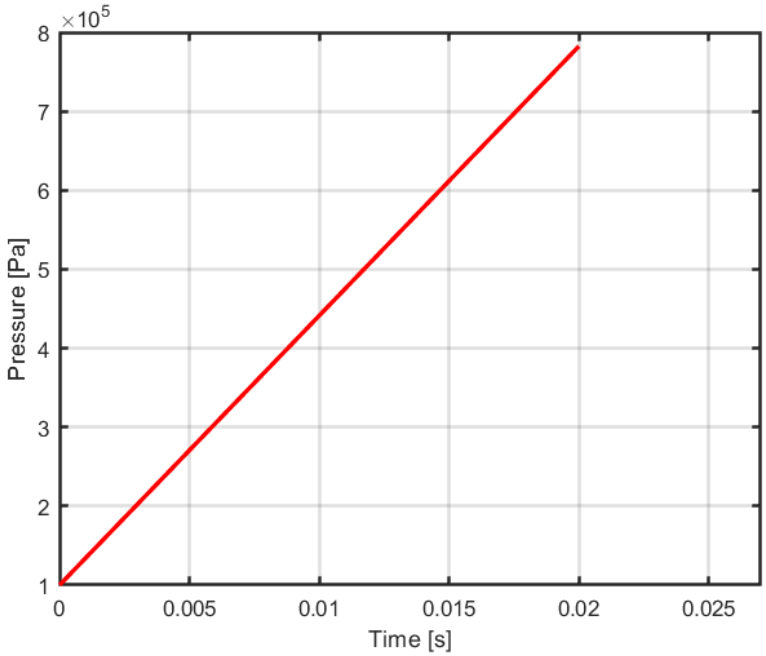

Figure 2: Combustion chamber pressure history.

	Inlet	Internal Field	Walls	Outlets
U (m/s)	zeroGradient	Uniform	noSlip	waveTransmissive
P (Pa)	totalPressure	Uniform	zeroGradient	waveTransmissive
T (K)	totalTemperature	Uniform	zeroGradient	waveTransmissive

Table 1: boundary condition.

Mesh Element Size	Total Cell Numbers
Finer Mesh (1.5 mm)	1955183
Fine Mesh (2 mm)	1108919
Medium Mesh (3 mm)	505343
Coarse Mesh (4 mm)	294115
Coarser Mesh (5 mm)	249473

Table 2: Mesh element size and total cell number.

2.1 Inviscid simulation results

Two different kinds of OpenFOAM compressible solvers are selected for inviscid simulations. sonicFoam and rhoCentralFoam, which can be arranged, respectively, as pressure-based and density-based solvers. In OpenFOAM, by making dynamic viscosity (mu) equal to zero, inviscid simulation can be conducted. In this paper, the verification study is based on inviscid model, and it is done for deflector with 45° angle. Combustion chamber total pressure varies with time. Inviscid simulations are conducted based on Nonomura el al. and Tsutsumi et al. combustion chamber total pressure history. In Housman et al study, combustion chamber total pressure values are higher than the Nonomura el al. and Tsutsumi et al. but for all the mentioned studies, the maximum total pressure value reaches 782500 Pa. Nonomura el al. and Tsutsumi et al. have studied the effect of IOP on sampling point No 10 and Housman et al studied the effect of IOP sampling point No 6 which is located on the wall (deflector).

Velocity contours from the rhoCentralFoam solver at 0.0035 and 0.009 seconds for the inviscid simulation are shown in Figures 3 and 4. Figure 5 compares the pressure history at sampling point No 10 from the present study with those from the studies by Nonomura et al. and Tsutsumi et al. Inviscid simulation results for the 45° deflector angle at sampling point No 10 are shown in Figures 6 and 7.

Sampling point No 6 is located on the wall (deflector) and its results are depicted in figures 8 and 9. Comparison of sonicFoam and rhoCentralFoam results for sampling point No 10 is shown in figure 10.

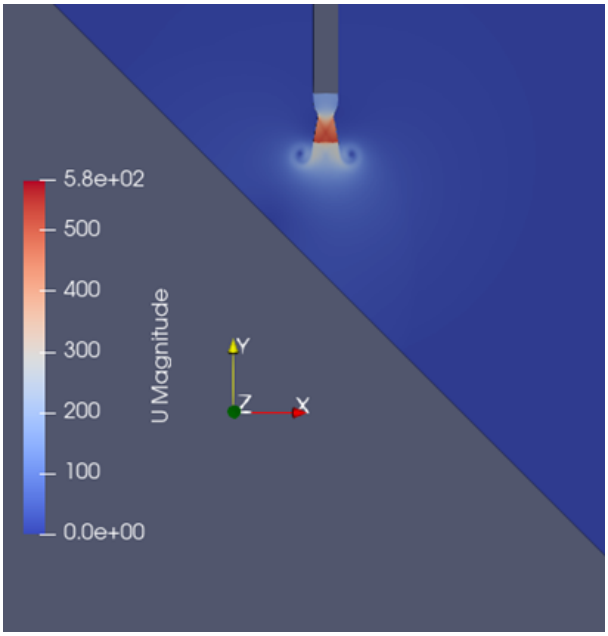

Figure 3: Velocity contour at 0.0035 second.

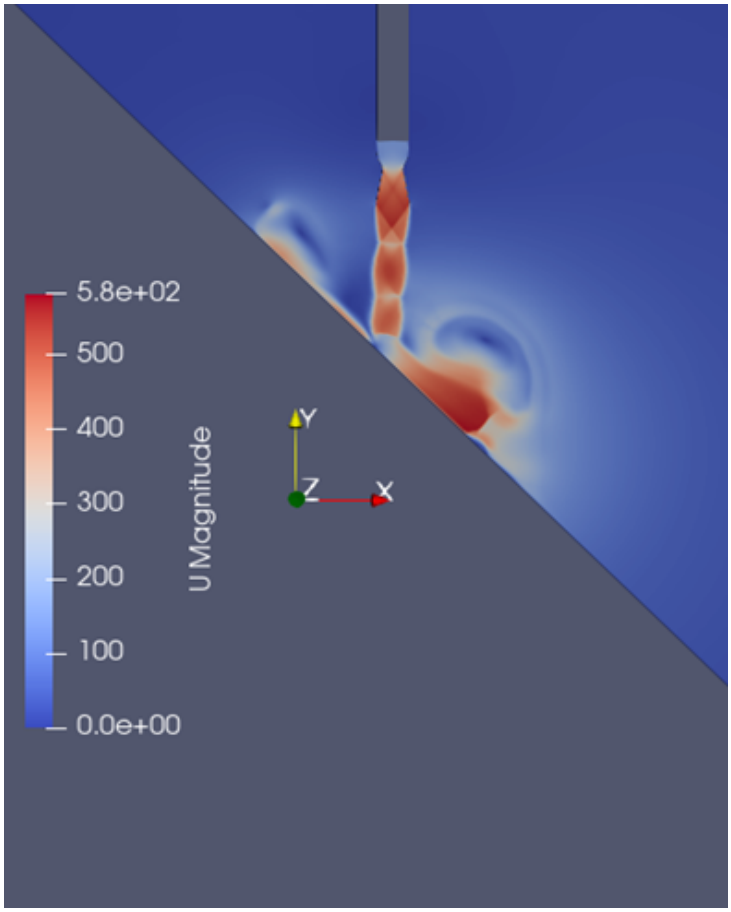

Figure 4: Velocity contour at 0.009 second.

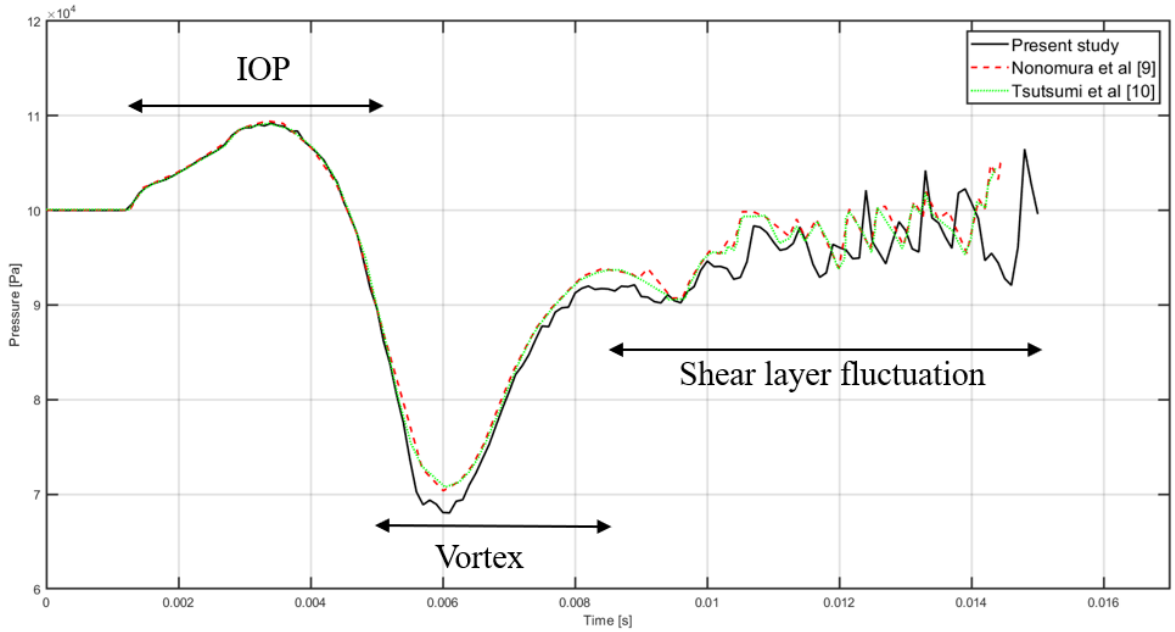

Figure 5: Sampling point No 10 pressure history obtained from inviscid solutions.

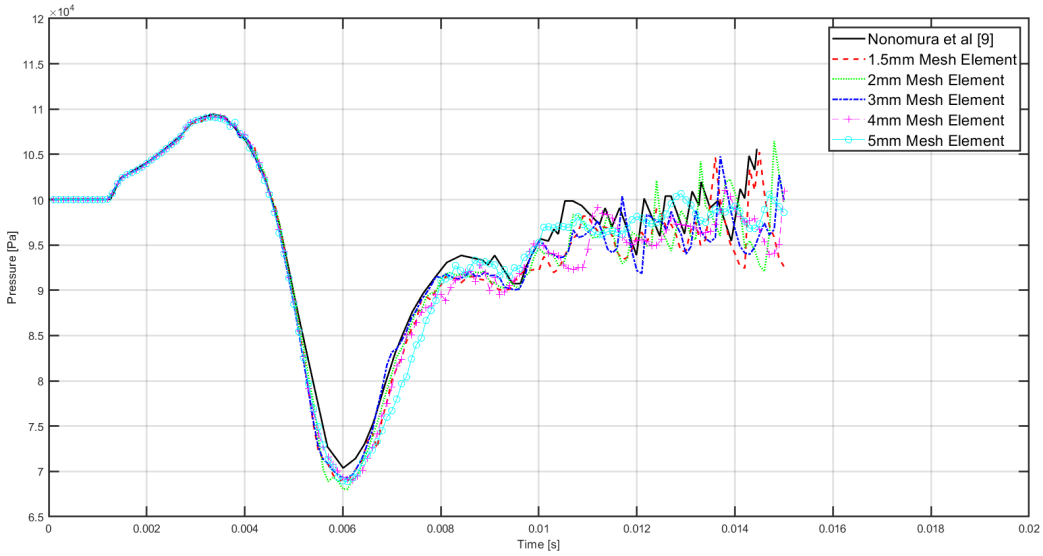

Figure 6: Sampling point No 10, pressure history obtained from inviscid simulation with sonicFoam (pressure-based) solver.

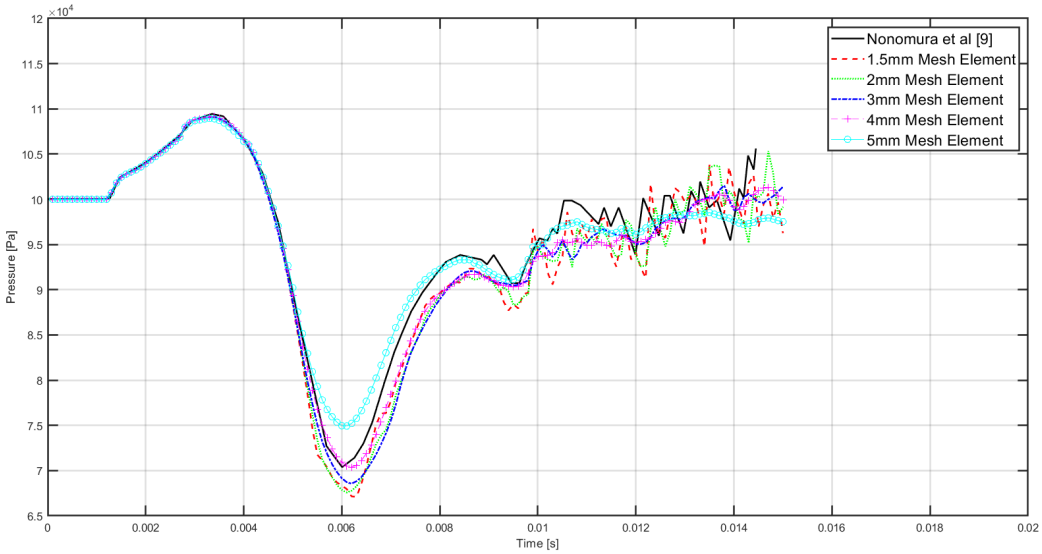

Figure 7: Sampling point No 10, pressure history obtained from inviscid simulation with rhoCentralFoam (density-based) solver.

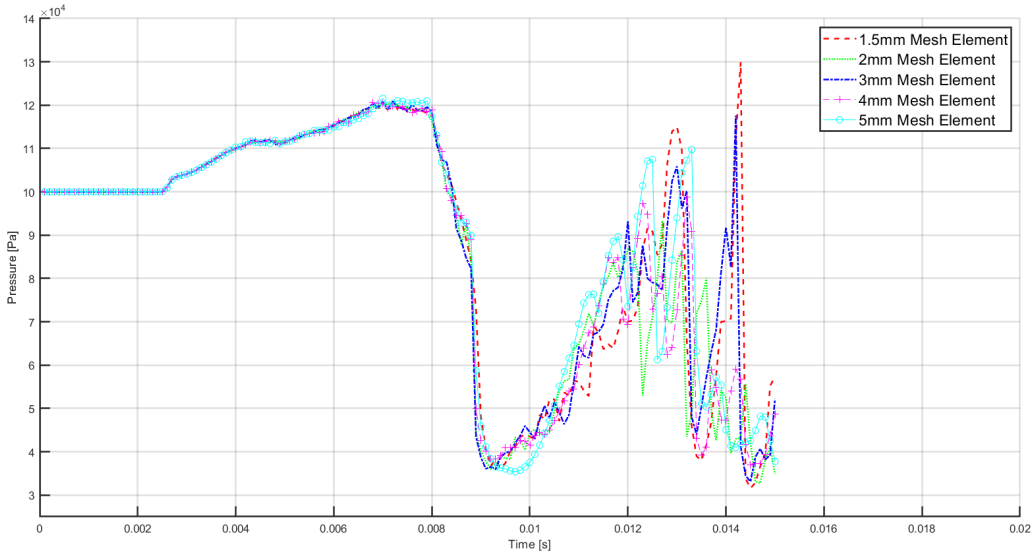

Figure 8: Sampling point No 6, pressure history obtained from inviscid simulation with sonicFoam (pressure-based) solver.

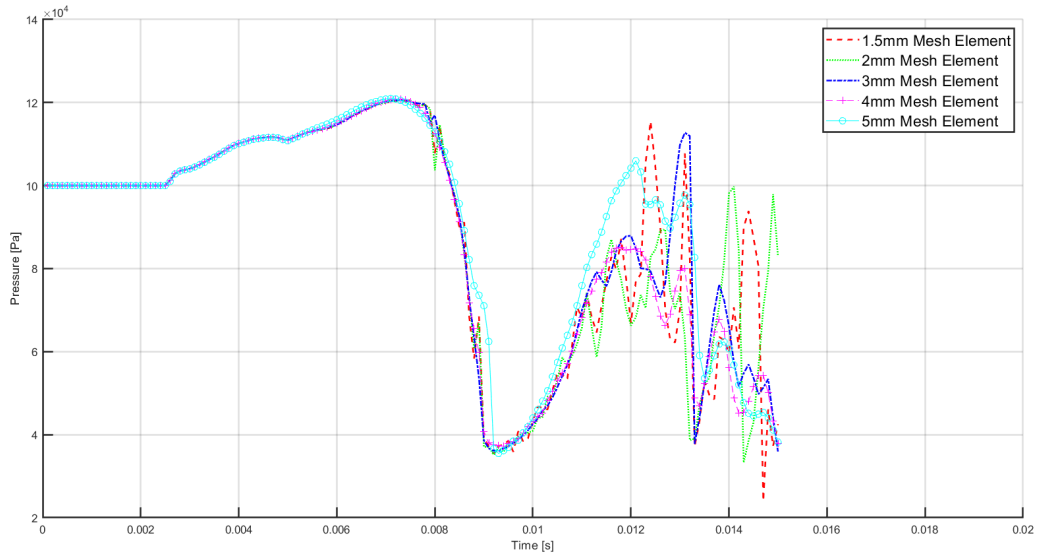

Figure 9: Sampling point No 6, pressure history obtained from inviscid simulation with rhoCentralFoam (pressure-based) solver.

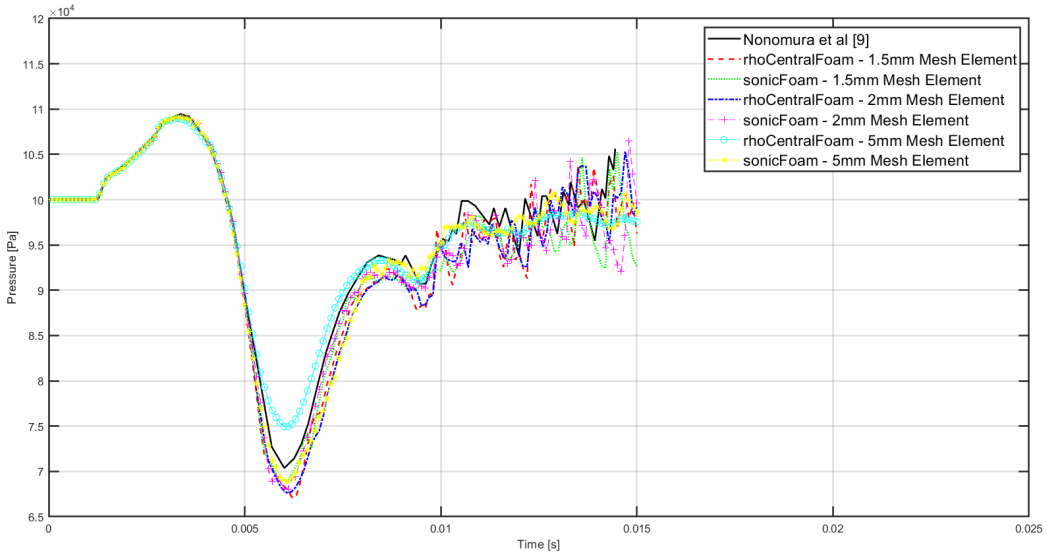

Figure 10: Comparing results of density-based and pressure-based solvers for sapling point No 10.

Housman et al. studied sampling point No 6, where the combustion chamber pressure history was higher compared to the studies by Nonomura et al. and Tsutsumi et al. In Housman et al. study with fine mesh at sampling point No 6, around 0.014 second maximum pressure fluctuation appeared. Approximate data digitization has been done for pressure history of sampling point No 6. Figure 11 compares sampling point No 6 the pressure history of the present study and the Housman et al study. In figure 11 it is seen that maximum pressure fluctuation in Housman et al. case is higher than in the present study. The results from sampling points No 10 and No 6 show that sonicFoam solver exhibits better performance and has more accuracy than the rhoCentralFoam solver. Therefore, the effect of wall angle variation on IOP is investigated using the sonicFoam solver with inviscid and turbulence models. In this study, deflector angles of 0°, 15°, 30°, and 60° were selected, and accordingly, a mesh element size of 2mm was generated for the flow domains. Figures 12 and 13 show the effect of deflector angle variation on IOP and the passing vortex using an inviscid solution.For sampling points No 10 and 6, by using inviscid solutions, the maximum values of IOP and negative pressure are observed for the 60° deflector angle. Increasing the deflector angle results in higher negative pressure values which is associated with the vortex. For both sampling points, increasing the deflector angle decreases the pressure fluctuations in the unresolved shear layer part.

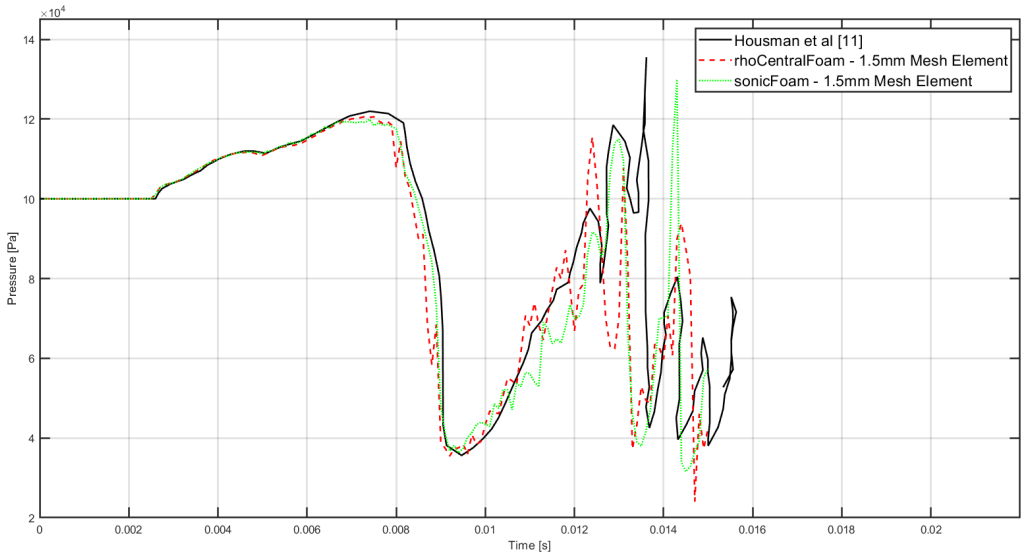

Figure 11: Comparison of inviscid results at sampling point No 6 between the present study and the Housman et al. case.

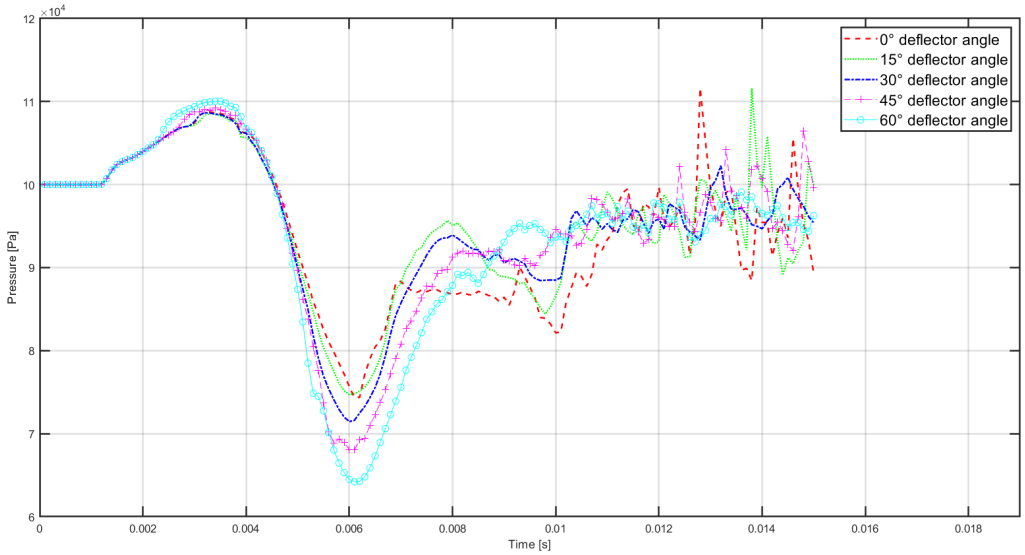

Figure 12: The effect of deflector angle variation on IOP and the passing vortex at sampling point No 10 using the sonicFoam solver.

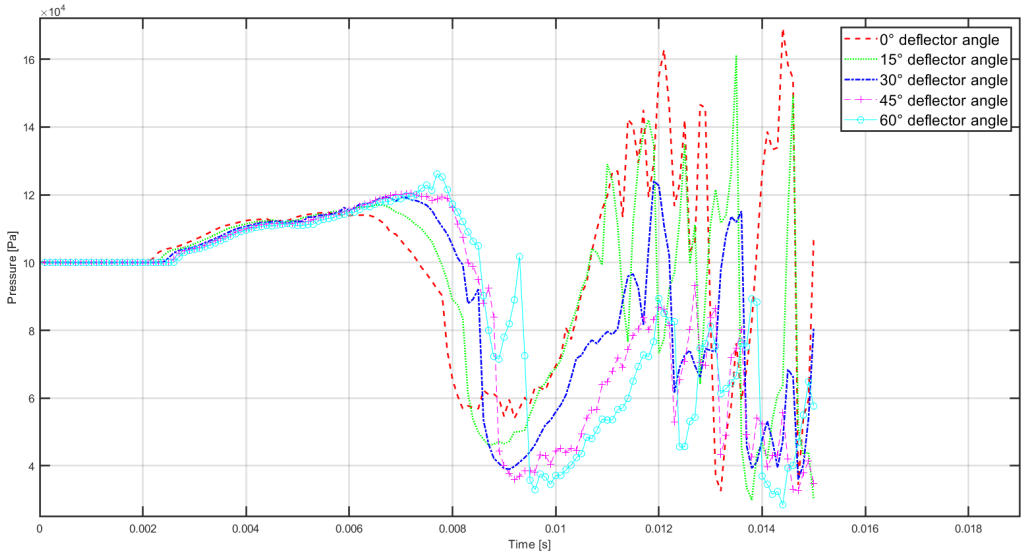

Figure 13: The effect of deflector angle variation on IOP and the passing vortex at sampling point No 6 using the sonicFoam solver.

2.2 kOmegaSST turbulence model simulation results

Based on the study by Tsutsumi et al., inviscid simulations can yield inaccurate results for pressure waves. In order to check the validity of the inviscid simulations, especially in wall regions, those results need to be compared with kOmegaSST turbulence model results. kOmegaSST is a two-equation eddy viscosity-based turbulence model which combines k-Epsilon and K-Omega turbulence models. It uses k-Epsilon for free shear layer and switches for K-Omega near wall regions [12]. The sonicFoam (pressure-based) solver has shown superior accuracy and stability compared to the rhoCentralFoam (density-based) solver. Therefore, it has been selected for conducting turbulence modeling. A mesh element size of 2mm is selected for the flow domain, similar to the inviscid domain mesh, with finer mesh near the wall regions (1mm mesh element size), and 40 boundary layers are added, which the first layer thickness is set to 5e-6m. Figures 14 and 15 show the results of the kOmegaSST turbulence model for sampling points No

10 and No 6. Comparison of inviscid and turbulence model results is conducted for each deflector angle and the results are shown in figures 16 to 25.For sampling points No 10 and 6, the kOmegaSST model solutions show that the maximum value of IOP is observed at a 60° deflector angle. By increasing the deflector angle value of negative pressure (related to vortex) increases at sampling point No 10. For both of the sampling points, by increasing of the deflector angle, the pressure fluctuation is decreasing in the unresolved shear layer part. Turbulence model boundary conditions are listed in table 3.

	Inlet	Internal Field	Walls	Outlets
U (m/s)	zeroGradient	Uniform	noSlip	waveTransmissive
P (Pa)	totalPressure	Uniform	zeroGradient	waveTransmissive
T (K)	totalTemperature	Uniform	zeroGradient	waveTransmissive
omega	fixedValue	Uniform	omegaWallFunction	zeroGradient
k	fixedValue	Uniform	kqRWallFunction	inletOutlet
nut	calculated	Uniform	nutkWallFunction	calculated
alphat	calculated	Uniform	compressible::alphatWallFunction	calculated

Table 3: Turbulence model boundary condition.

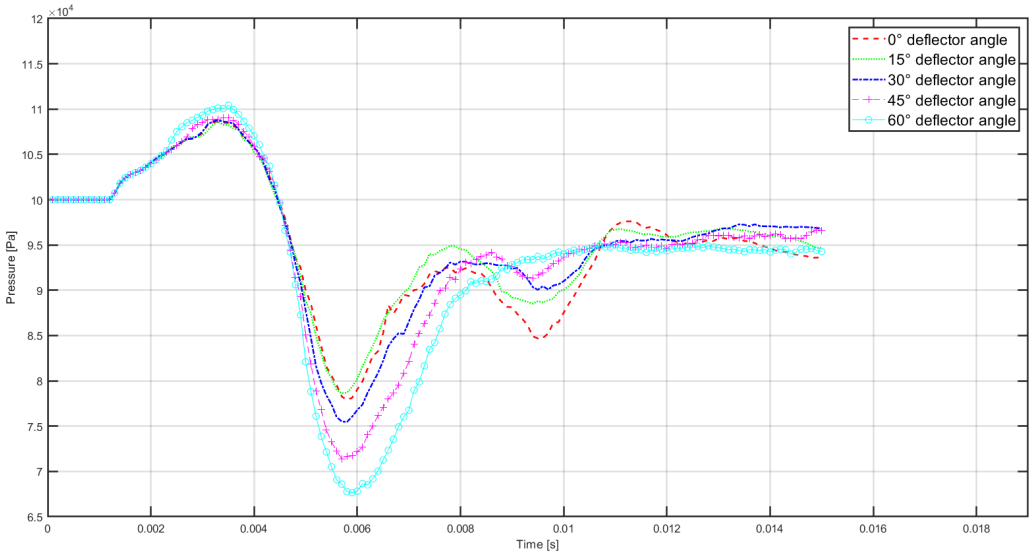

Figure 14: Effect of deflector angle on IOP and vortex (simulated using sonicFoam with kOmegaSST model) for sampling point No 10.

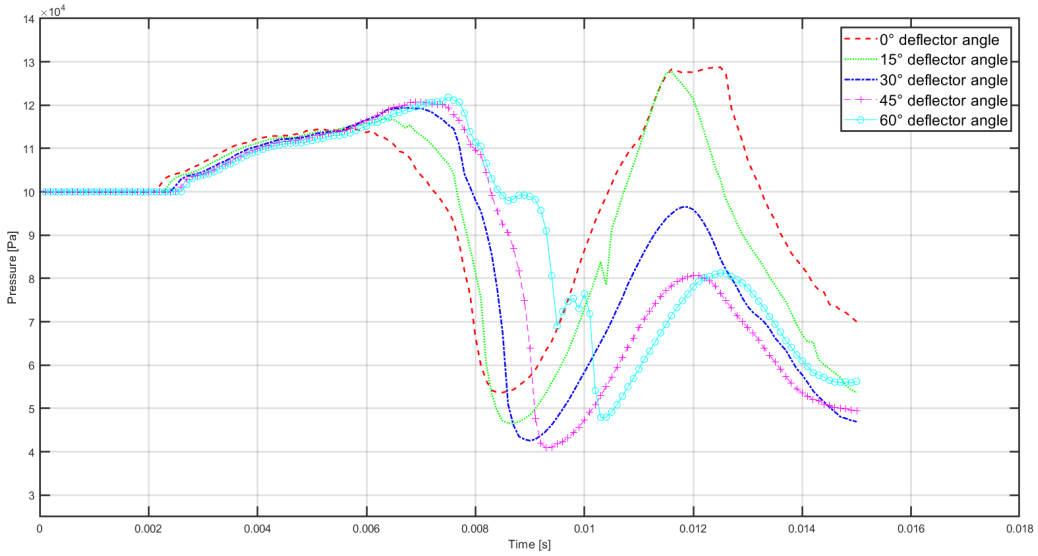

Figure 15: Effect of deflector angle on IOP and vortex (simulated using sonicFoam with kOmegaSST model) for sampling point No 6.

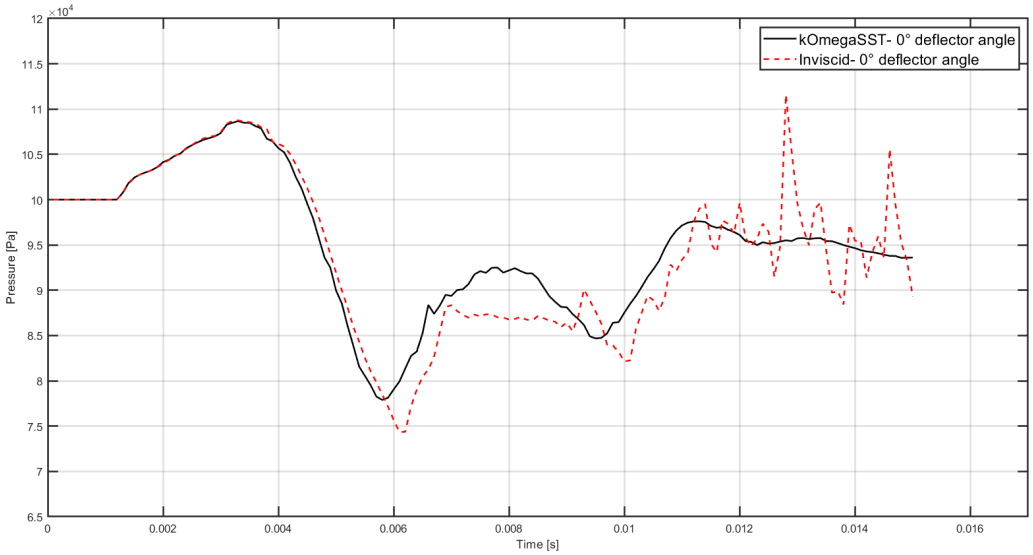

Figure 16: Comparison of inviscid and kOmegaSST models results for sampling point No 10 at a 0° deflector angle using the sonicFoam solver.

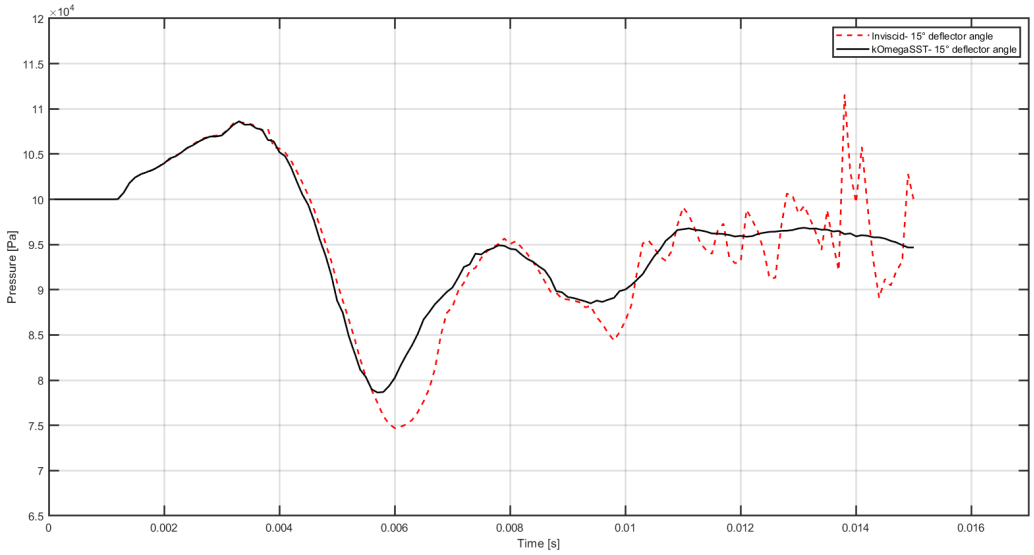

Figure 17: Comparison of inviscid and kOmegaSST results for sampling point No 10 at a 15° deflector angle using the sonicFoam solver.

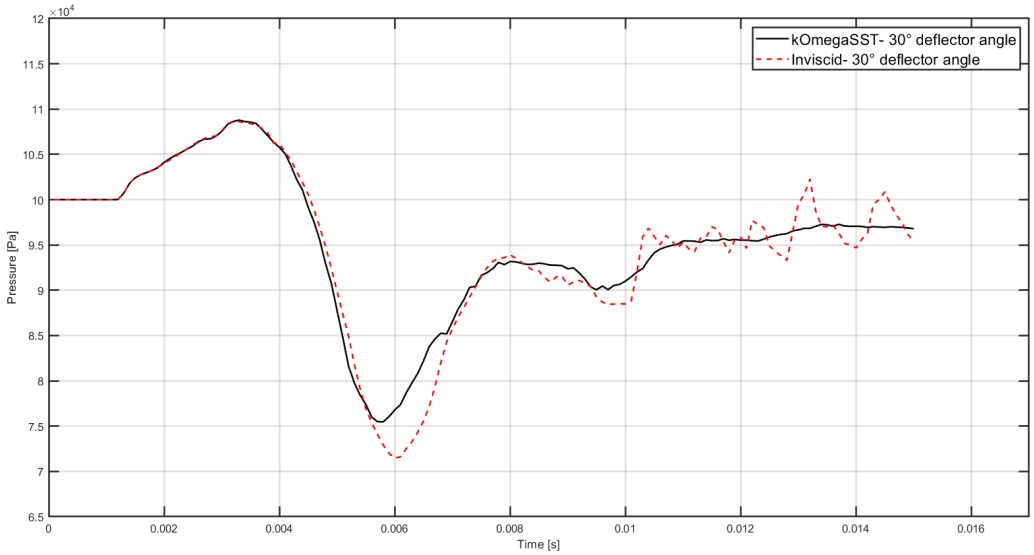

Figure 18: Comparison of inviscid and kOmegaSST results for sampling point No 10 at a 30° deflector angle using the sonicFoam solver.

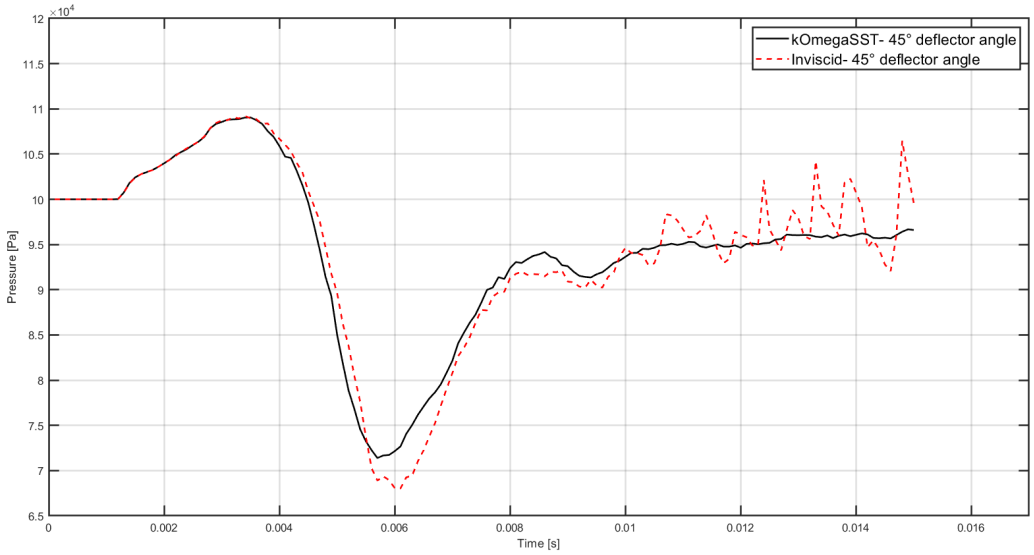

Figure 19: Comparison of inviscid and kOmegaSST results for sampling point No 10 at a 45° deflector angle using the sonicFoam solver.

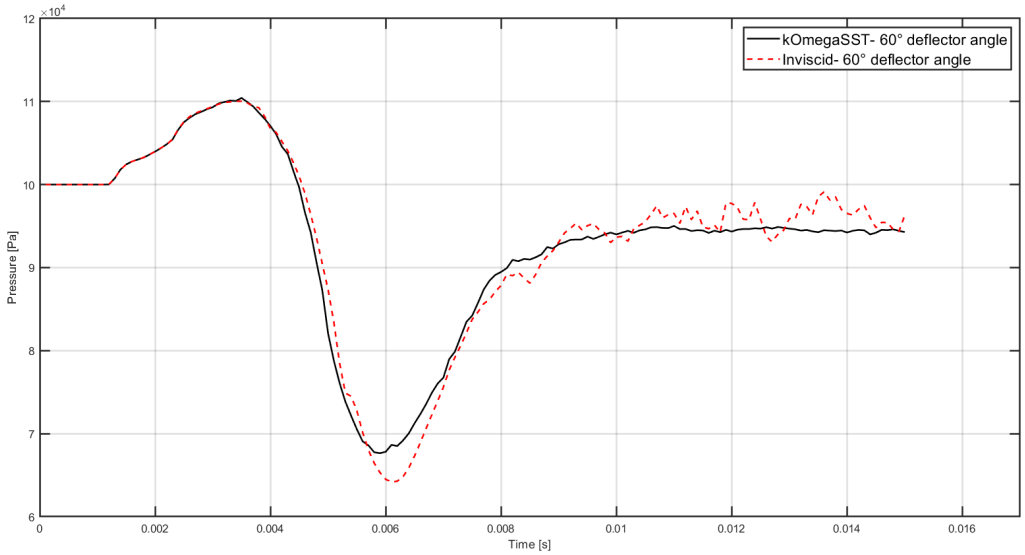

Figure 20: Comparison of inviscid and kOmegaSST results for sampling point No 10 at a 60° deflector angle using the sonicFoam solver.

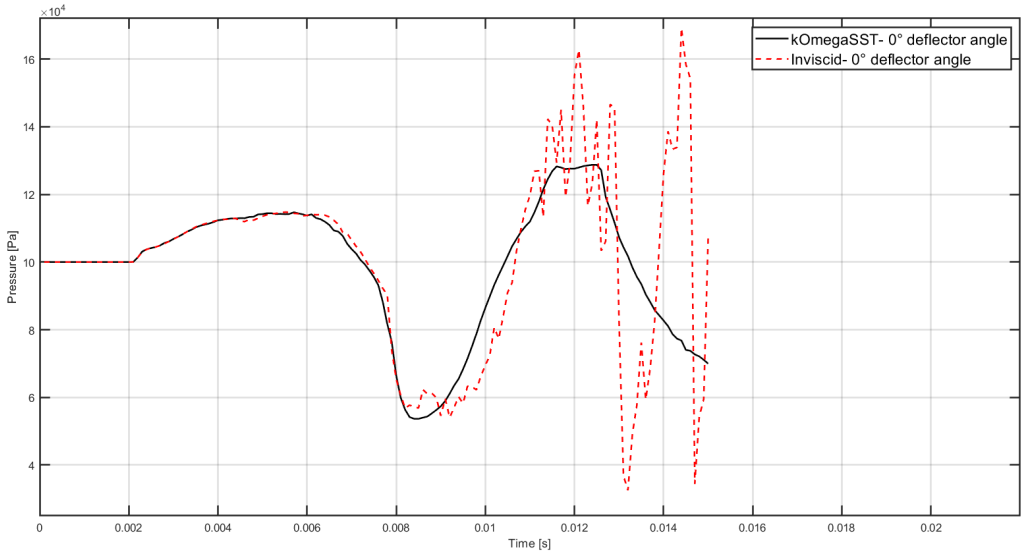

Figure 21: Comparison of inviscid and kOmegaSST results for sampling point No 6 at a 0° deflector angle using the sonicFoam solver.

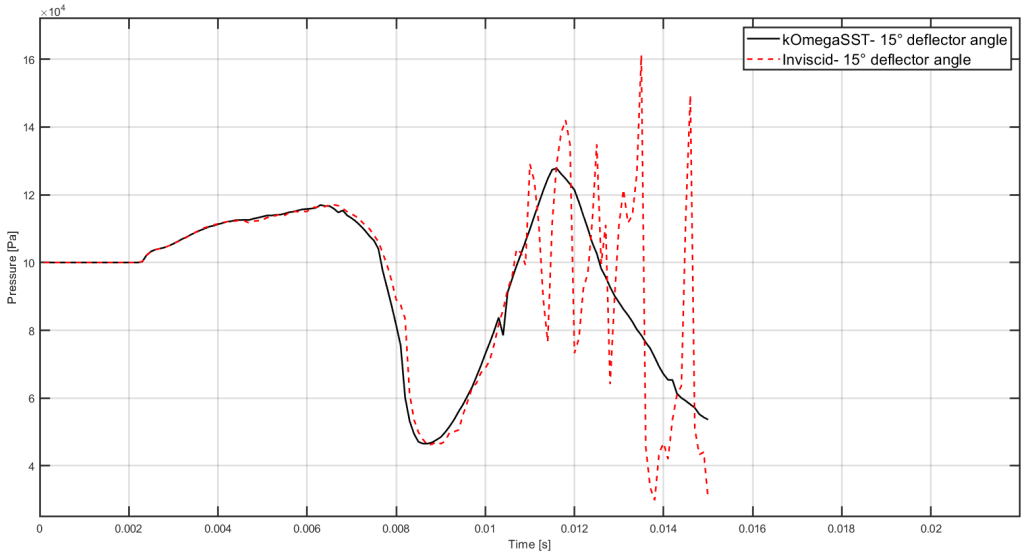

Figure 22: Comparison of inviscid and kOmegaSST results for sampling point No 6 at a 15° deflector angle using the sonicFoam solver.

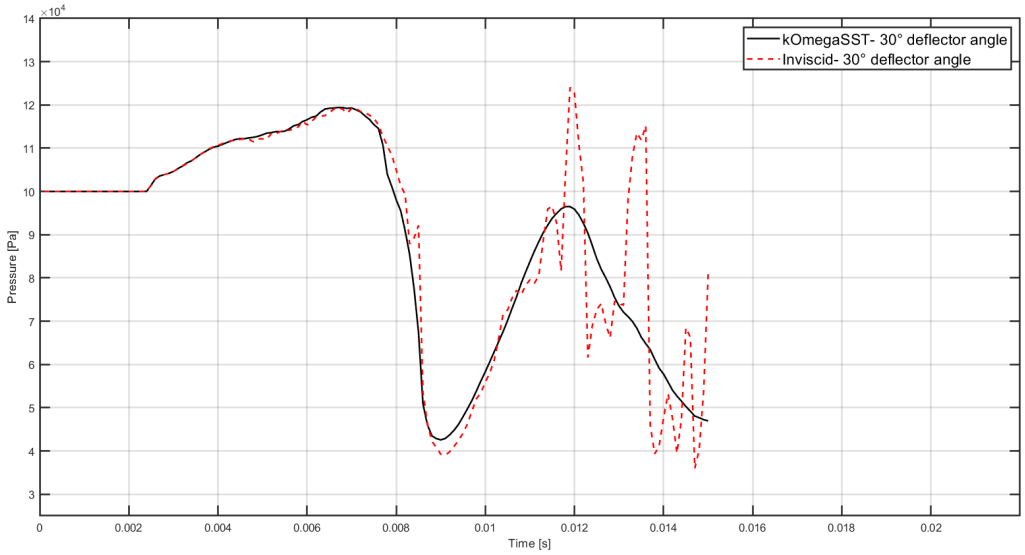

Figure 23: Comparison of inviscid and kOmegaSST results for sampling point No 6 at a 30° deflector angle using the sonicFoam solver.

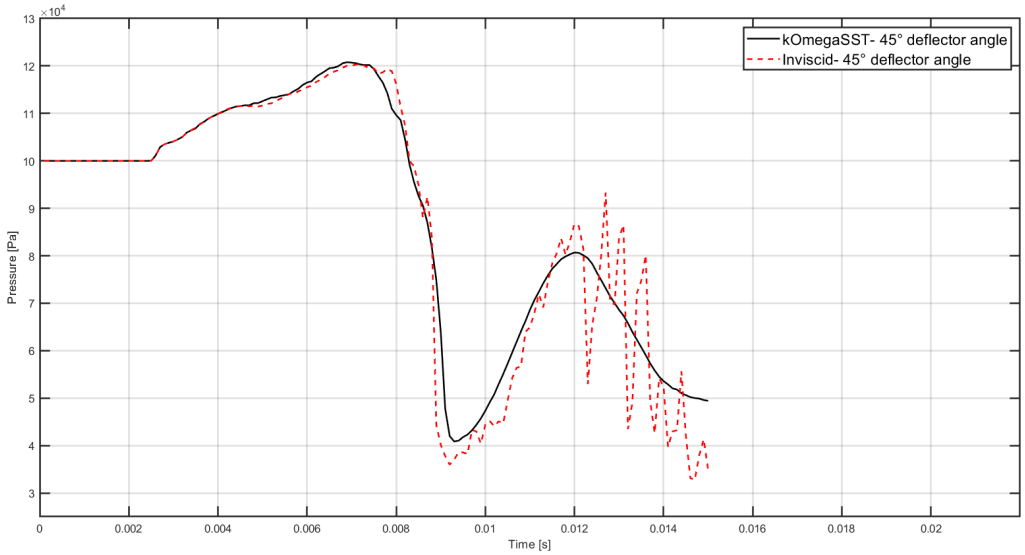

Figure 24: Comparison of inviscid and kOmegaSST results for sampling point No 6 at a 45° deflector angle using the sonicFoam solver.

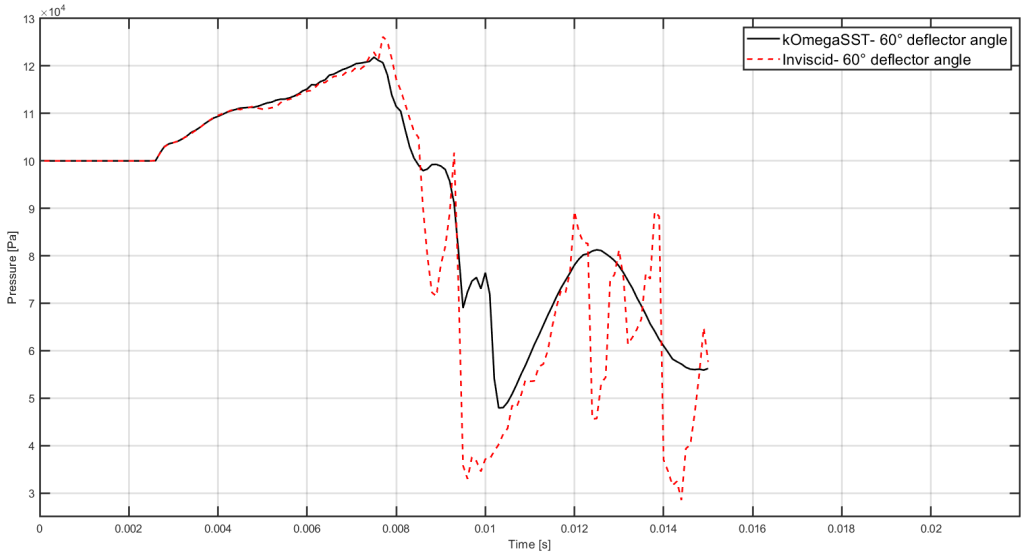

Figure 25: Comparison of inviscid and kOmegaSST results for sampling point No 6 at a 60° deflector angle using the sonicFoam solver.

Flow field and velocity contours at 0.01 second for deflector angles of 0°, 15°, 30°, 45°, and 60°, obtained from inviscid and kOmegaSST turbulence model simulations using the sonicFoam solver, are shown in Figures 26 to 35.

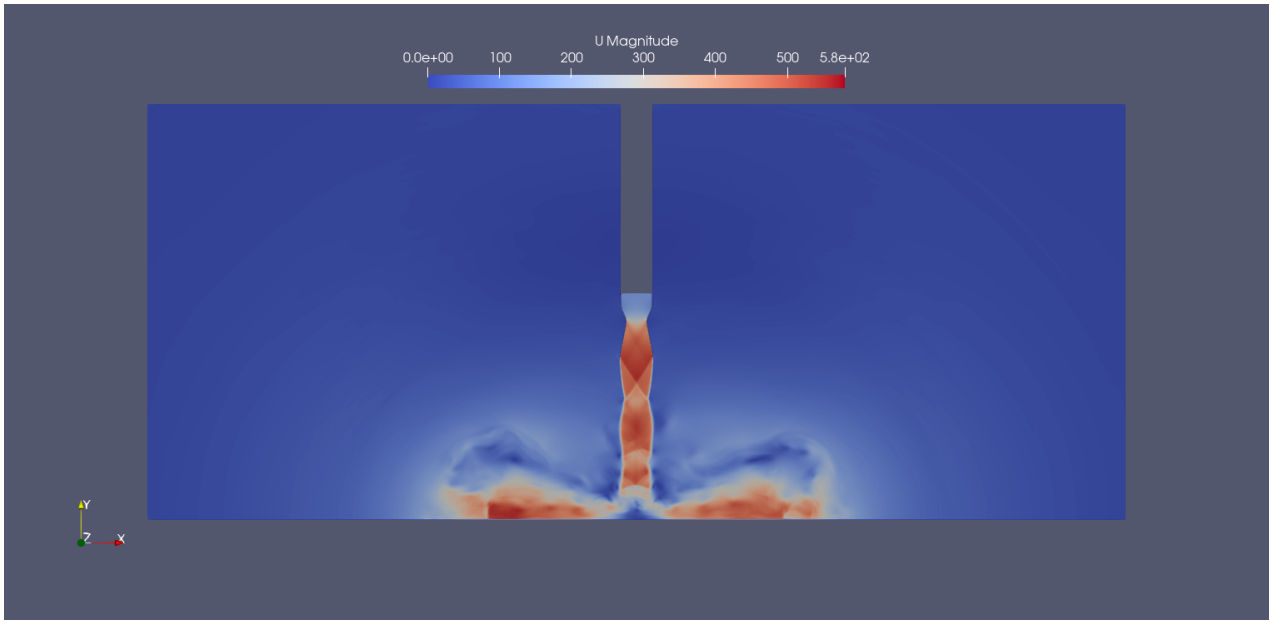

Figure 26: Velocity contour at 0.01 second for the inviscid simulation with a 0° deflector angle.

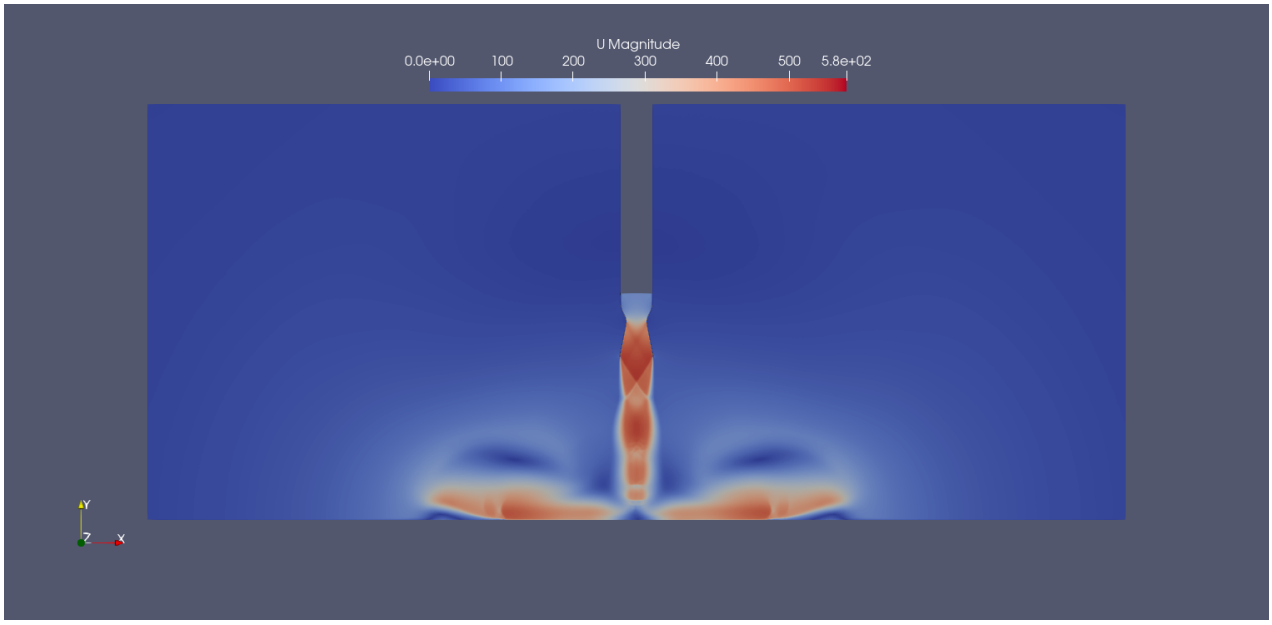

Figure 27: Velocity contour at 0.01 second for the kOmegaSST simulation with a 0° deflector angle.

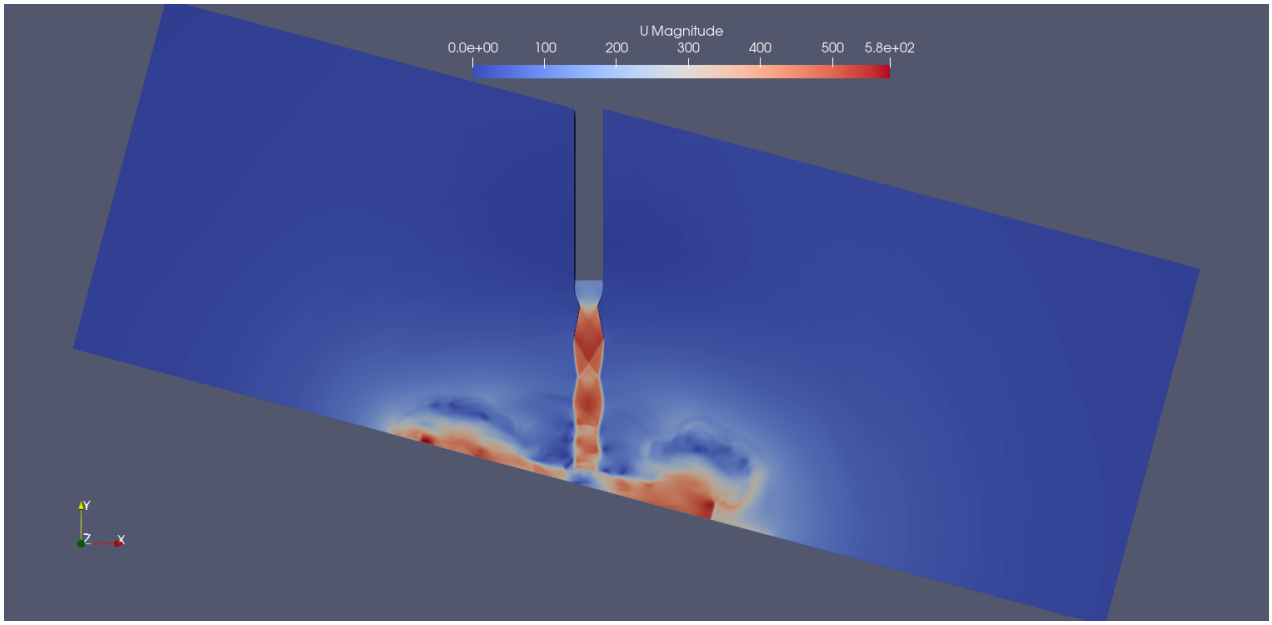

Figure 28: Velocity contour at 0.01 second for the inviscid simulation with a 15° deflector angle.

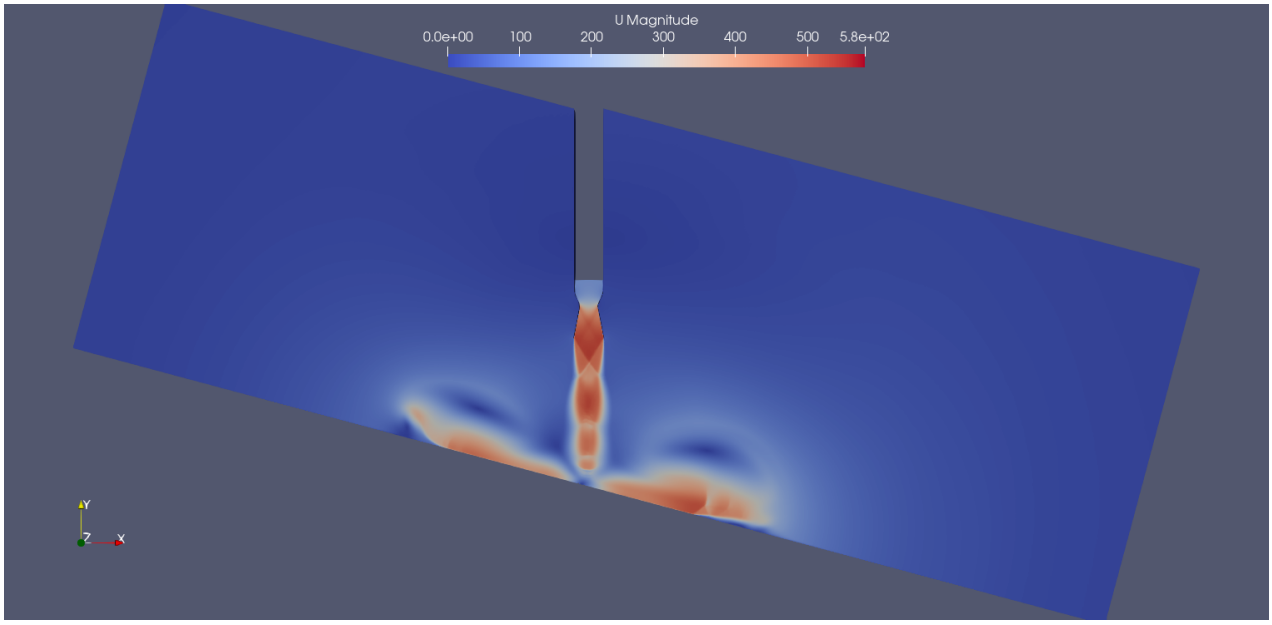

Figure 29: Velocity contour at 0.01 second for the kOmegaSST simulation with a 15° deflector angle.

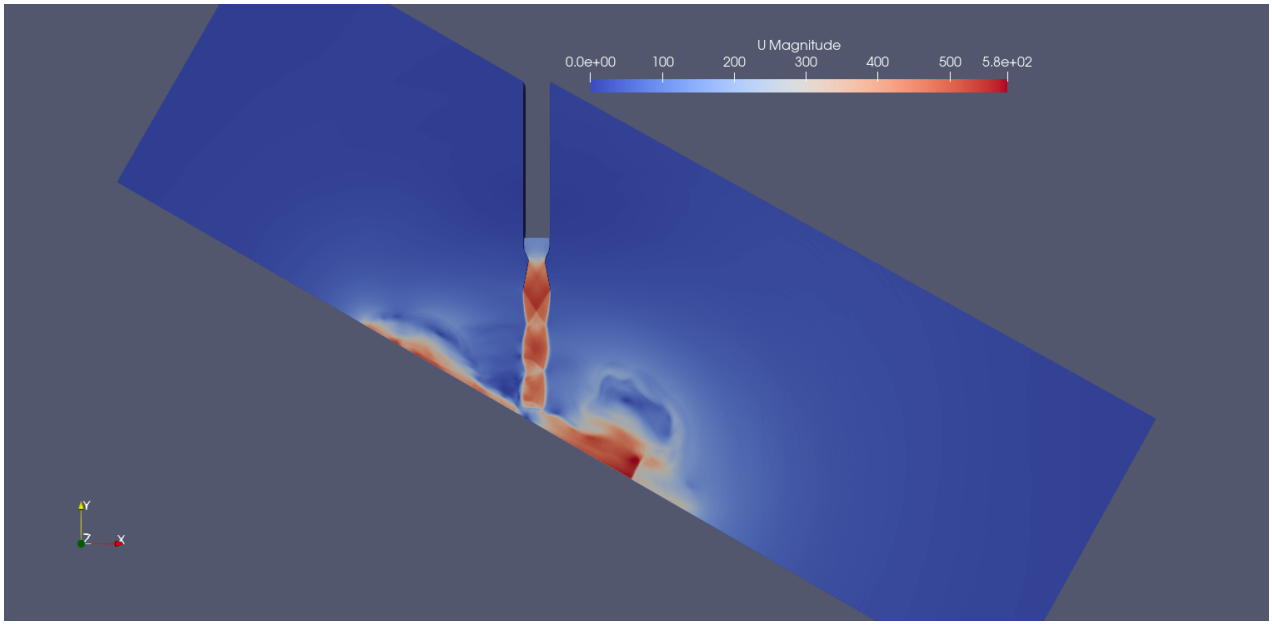

Figure 30: Velocity contour at 0.01 second for the inviscid simulation with a 30° deflector angle.

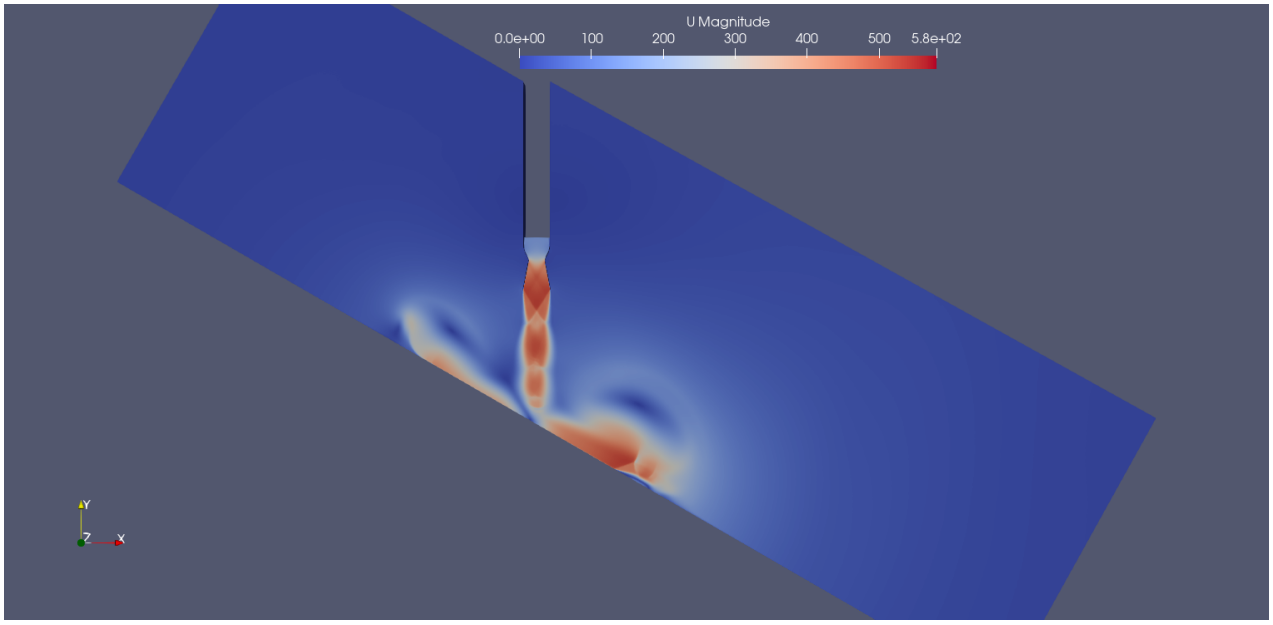

Figure 31: Velocity contour at 0.01 second for the kOmegaSST simulation with a 30° deflector angle.

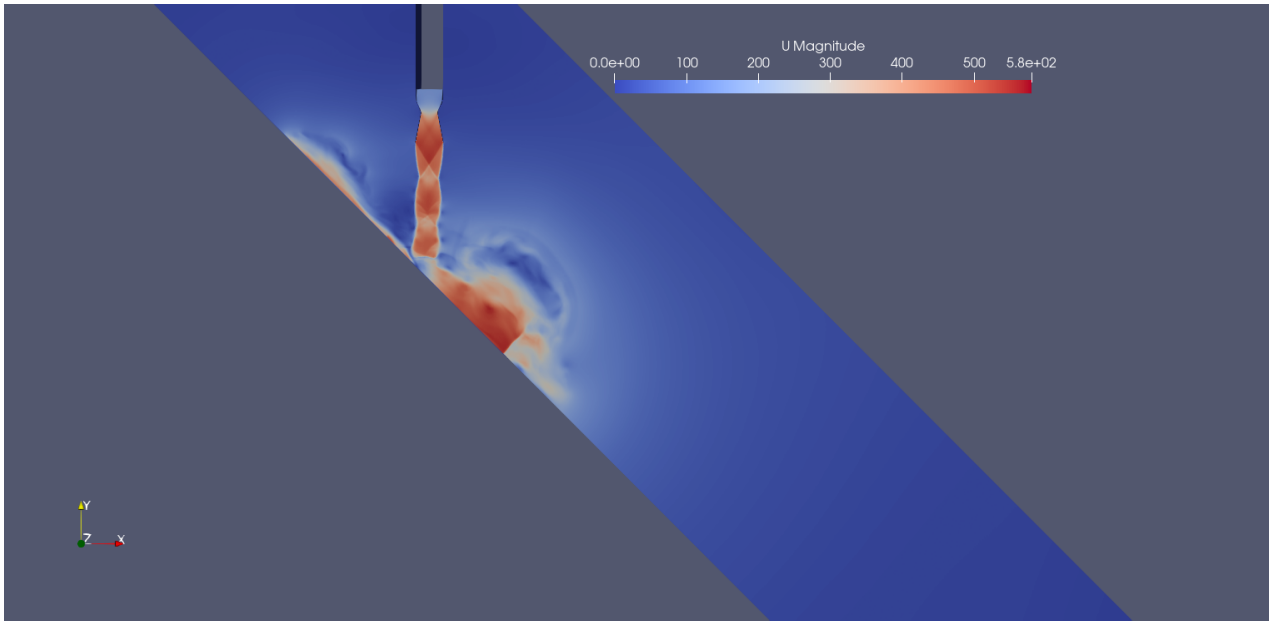

Figure 32: Velocity contour at 0.01 second for the inviscid simulation with a 45° deflector angle.

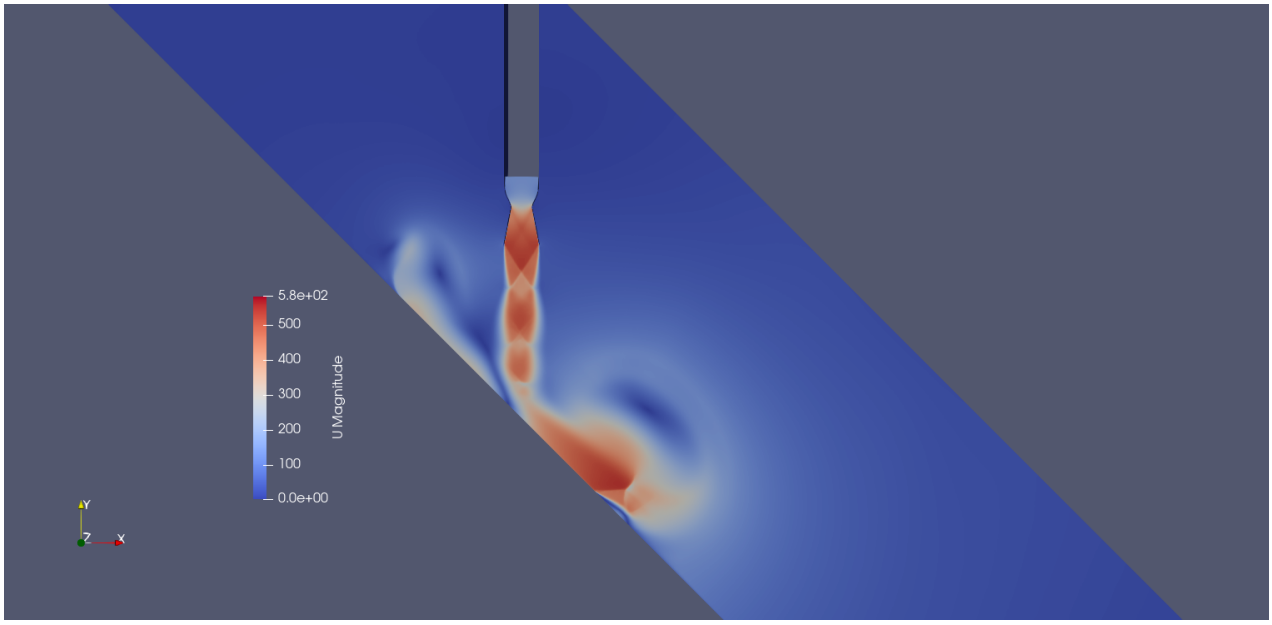

Figure 33: Velocity contour at 0.01 second for the kOmegaSST simulation with a 45° deflector angle.

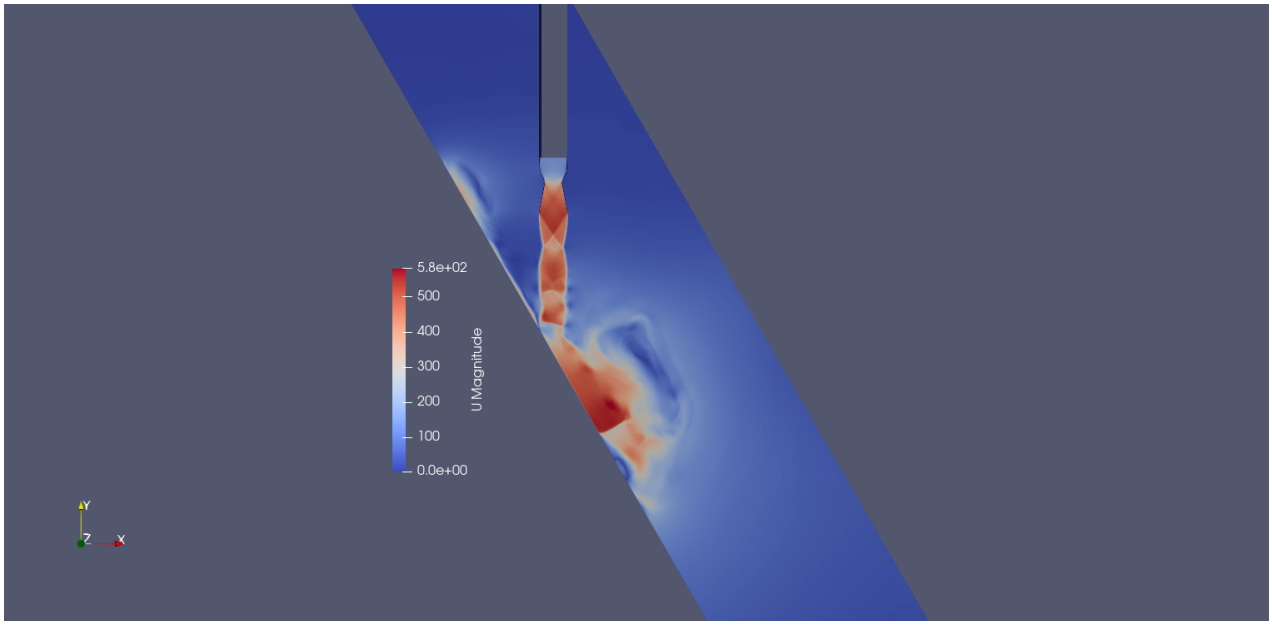

Figure 34: Velocity contour at 0.01 second for the inviscid simulation with a 60° deflector angle.

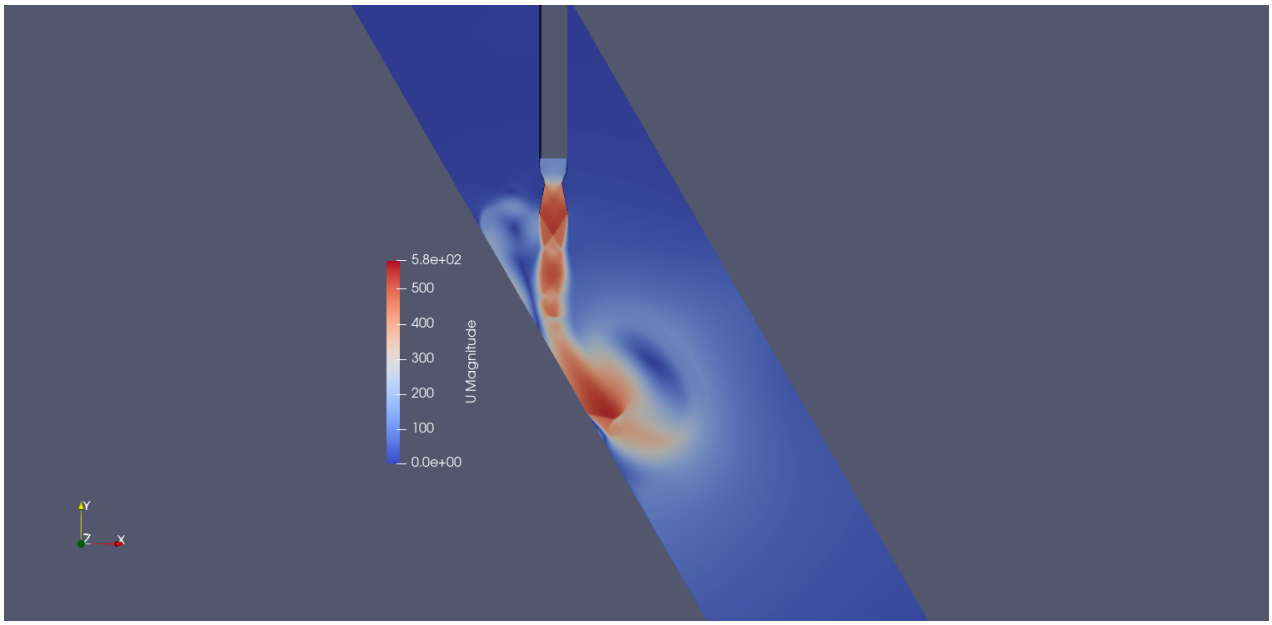

Figure 35: Velocity contour at 0.01 second for the kOmegaSST simulation with a 60° deflector angle.

By comparing figures 26 to 35 it can be concluded that kOmegaSST turbulence model accurately represents flow details. By increasing deflector angle, circulation becomes stronger and it can direct flow back toward launch vehicle at higher deflector angles. At 0.01 second, for 60° deflector angle, the flow circulation has reached the nozzle. Higher deflector angles generate more negative pressure and pose a risk of directing back flow toward the launch vehicle.

3 Conclusion and Future Work

The aim of this study is the CFD analysis of Ignition Over-Pressure (IOP). IOP is an unsteady pressure wave which appears during ignition of launch vehicles rockets. This unsteady phenomenon can have destructive effects on the structures and on launch vehicles. In order to have safe launch, IOP should be analyzed and reduced. In this study the effects of deflector wall angles on IOP waves are investigated using both inviscid and viscous models. A numerical verification study is conducted using OpenFOAM compressible solvers. Specifically, rhoCentralFoam (density-based) and sonicFoam (pressure-based) solvers are selected for this study. The results of inviscid simulations show that the sonicFoam solver exhibits more accuracy than the rhoCentralFoam solver. Therefore, it has been selected to investigate the effect of deflector angle variation on the IOP. After numerical verification, the effect of deflector angle on IOP was studied by individually analyzing deflector angles of 0°, 15°, 30°, 45°, and 60° using inviscid and viscous simulations, and comparing their results. In this study, there are two sampling points: one near the nozzle exit (point No 10) and the other on the wall (point No 6). At sampling points No 10 and 6, the inviscid solutions show that the maximum value of IOP and maximum negative pressure are observed at a 60° deflector angle. By increasing deflector angle value of negative pressure (related to vortex) increases. For both sampling points, increasing the deflector angle results in a decrease in pressure fluctuation within the unresolved shear layer. At sampling points No 10 and 6, kOmegaSST turbulence model solutions indicate that the maximum value of IOP is observed at a 60° deflector angle. Viscous solutions indicate that by increasing the deflector angle, value of negative pressure (related to vortex) increases at sampling point No 10. Additionally, at sampling point No 6, the negative pressure (related to the vortex) increases as the deflector angle is increased from 0° to 45°, and then decreases at a 60° deflector angle. For both of the sampling points, by increasing deflector angle, the pressure fluctuation is decreasing in the unresolved shear layer. Comparison of inviscid and turbulence model solutions shows good agreement in predicting IOP, especially for the maximum positive pressure value. The results indicate that pressure fluctuations in the shear layer are higher for inviscid solutions. There is a difference in the prediction of maximum negative pressure (vortex) between inviscid and viscous models. The viscous model (kOmegaSST turbulence model) accurately provides flow details compared to the inviscid model. After the flow impinges on the deflector (wall), flow circulation appears. As the deflector

angle increases, the flow circulation becomes stronger and can direct flow back toward the launch vehicle at higher deflector angles. At 0.01 seconds, for 60° deflector, the flow circulation has reached the nozzle. Higher deflector angles result in higher negative pressure values and can have risk of back flow reaching the launch vehicle. The deflector angle should be selected to minimize IOP values, prevent flow back toward the launch vehicle (minimize negative pressure), and reduce pressure fluctuations in the shear layer. In future study, the effect of impinging distance on (IOP) will be investigated.

4 Acknowledgment

This study was funded by the Scientific and Technological Research Council of Turkey (TUBITAK). ARDEB 1001 Grant No 123M355.

References

[1] Donald K Nance and Peter A Liever. Space launch system scale model acoustic test ignition overpressure testing. In *Aerospace Testing Conference*, number M15-4899, 2015.

[2] Raoul E Caimi, Ravi N Margashayam, Jamal F Nayfeh, and Karen Thompson. Rocket launch-induced vibration and ignition overpressure response. In *ICSV8 International Congress on Sound and Vibration*, 2001.

[3] Francisco Canabal and Abdelkader Frendi. Study of the ignition overpressure suppression technique by water addition. *Journal of spacecraft and rockets*, 43(4):853–865, 2006.

[4] Chenyu Lu, Zhitan Zhou, Yue Shi, Yiying Bao, and Guigao Le. Numerical simulations of water spray on launch pad during rocket launching. *Journal of Spacecraft and Rockets*, 58(2):566–574, 2021.

[5] Zhitan Zhou, Liangjun Zhang, and Guigao Le. Numerical study for the flame deflector design of four-engine liquid rockets. *Engineering Applications of Computational Fluid Mechanics*, 14(1):726–737, 2020.

[6] EJ Walsh and PM Hart. Liftoff ignition overpressure-a correlation. *Journal of Spacecraft and Rockets*, 19(6):550–556, 1982.

[7] Danny Pavish and Jerry Deese. Cfd analysis of unsteady ignition overpressure effects on delta ii and iii launch vehicles. In *18th Applied Aerodynamics Conference*, page 3922, 2000.

[8] Bernard Troclet, S Alestra, I Terrasse, S Jeanjean, and Vassili Srithammavanh. Identification of overpressure sources at launch vehicle liftoff using an inverse method. *Journal of Spacecraft and Rockets*, 44(3):597–606, 2007.

[9] T Nonomura, S Tsutsumi, R Takaki, E Shima, and K Fujii. Impact of temporal and spatial resolution on the aeroacoustic waves from a two-dimensional impinging jet. In *7th International Conference on Computational Fluid Dynamics (ICCFD7), Paper ICCFD7-3103, Big Island, Hawaii*, 2012.

[10] Seiji Tsutsumi, Ryoji Takaki, Toshiaki Hara, Hiroyuki Ueda, and Hiroyuki Nagata. Numerical analysis of ignition overpressure effect on h-iib launch vehicle. *Journal of Spacecraft and Rockets*, 51(3):893–899, 2014.

[11] Jeffrey Housman, Michael Barad, and Cetin Kiris. Space-time accuracy assessment of cfd simulations for the launch environment. In *29th AIAA Applied Aerodynamics Conference*, page 3650, 2011.

[12] Florian R Menter. Two-equation eddy-viscosity turbulence models for engineering applications. *AIAA journal*, 32(8):1598–1605, 1994.